where

$$
\begin{aligned}
Den1 =&\mu_3\gamma_1\cosh(\gamma_1h_1)\cosh(\gamma_2h_2)\sinh(\gamma_3h_3)\\
&+\frac{\mu_2\gamma_1\gamma_3}{\gamma_2}\cosh(\gamma_1h_1)\sinh(\gamma_2h_2)\cosh(\gamma_3h_3)\\
&+\mu_1\gamma_3\sinh(\gamma_1h_1)\cosh(\gamma_2h_2)\cosh(\gamma_3h_3)\\
&+\frac{\mu_1\mu_3}{\mu_2\gamma_2}\sinh(\gamma_1h_1)\sinh(\gamma_2h_2)\sinh(\gamma_3h_3)\\
Den2 =&\epsilon_3\gamma_1\sinh(\gamma_1h_1)\cosh(\gamma_2h_2)\cosh(\gamma_3h_3)\\
&+\frac{\epsilon_2\gamma_1\gamma_3}{\gamma_2}\sinh(\gamma_1h_1)\sinh(\gamma_2h_2)\sinh(\gamma_3h_3)\\
&+\epsilon_1\gamma_3\cosh(\gamma_1h_1)\cosh(\gamma_2h_2)\sinh(\gamma_3h_3)\\
&+\frac{\epsilon_1\epsilon_3\gamma_2}{\epsilon_2}\cosh(\gamma_1h_1)\sinh(\gamma_2h_2)\cosh(\gamma_3h_3)\\
f_{22} =&\frac{\epsilon_1}{\mu_3}\cosh(\gamma_1h_1)\cosh(\gamma_2h_2)\cosh(\gamma_3h_3)\\
&+\frac{\epsilon_3\gamma_1}{\mu_3\gamma_3}\sinh(\gamma_1h_1)\cosh(\gamma_2h_2)\sinh(\gamma_3h_3)\\
&+\frac{\epsilon_2\gamma_1}{\mu_3\gamma_2}\sinh(\gamma_1h_1)\sinh(\gamma_2h_2)\cosh(\gamma_3h_3)\\
&+\frac{\epsilon_1\epsilon_3\gamma_2}{\epsilon_2\mu_3\gamma_3}\cosh(\gamma_1h_1)\sinh(\gamma_2h_2)\sinh(\gamma_3h_3)\\
g_{22} =&\gamma_3\left(\frac{\mu_1\epsilon_1\epsilon_3}{\mu_2\epsilon_2}-\epsilon_3\right)\sinh\gamma_1h_1\cosh\gamma_1h_1\\
&+\gamma_3\left(\frac{\mu_1\epsilon_1}{\mu_3}-\frac{\epsilon_1\epsilon_3\mu_1}{\mu_2\epsilon_2}\right)\cosh\gamma_1h_1\sinh\gamma_1h_1\cosh^2\gamma_2h_2\\
&+\frac{\gamma_1^2\gamma_3}{\gamma_2^2}\left(\frac{\mu_2\epsilon_2}{\mu_3}-\epsilon_3\right)\sinh\gamma_1h_1\cosh\gamma_1h_1\sinh^2\gamma_2h_2\\
&+\frac{\gamma_3\gamma_1}{\gamma_2}\left(\frac{\mu_1\epsilon_2}{\mu_3}-\frac{\mu_1\epsilon_3}{\mu_2}\right)\sinh^2\gamma_1h_1\cosh\gamma_2h_2\sinh\gamma_2h_2\\
&+\frac{\gamma_3\gamma_1}{\gamma_2}\left(\frac{\mu_2\epsilon_1}{\mu_3}-\frac{\epsilon_1\epsilon_3}{\epsilon_2}\right)\cosh^2\gamma_1h_1\cosh\gamma_2h_2\sinh\gamma_2h_2.
\end{aligned}
$$

References

[1] J. W. Greiser, "Coplanar stripline antenna," *Microwave J.*, pp. 47-49, Oct. 1976.

[2] A. Nešić, "Bandwidth and radiation characteristics of the printed slot excited by a coplanar waveguide," in *Proc. Third Int. Conf. Antennas Propagat. ICAP 83,* 1983, pp. 404–406.

[3] W. Menzel and W. Grabherr, "A microstrip patch antenna with coplanar feed line," *IEEE Microwave Guided Wave Lett.*, vol. 1, no. 11, pp. 340–342, Nov. 1991.

[4] H. C. Liu, T. S. Horng, and N. G. Alexopoulos, "Radiation from aperture antennas with a coplanar waveguide feed," *1992 IEEE AP-S Symp. Dig.*, pp. 1820–1823.

[5] J. Litva, C. Wu, Z. Bi, and K. Wu, "Some considerations for microstrip coplanar-waveguide antennas," *1992 IEEE AP-S Symp. Dig.*, pp. 491–494.

[6] R. N. Simons and R. Q. Lee, "Coplanar waveguide aperture coupled patch antennas with ground plane/substrate of finite extent," *Electron. Lett.*, vol. 28, no. 1, pp. 75–76, Jan. 2, 1992.

[7] R. Q. Lee and R. N. Simons, "Coplanar waveguide aperture coupled microstrip patch antenna," *IEEE Microwave Guided Wave Lett.*, vol. 2, no. 4, pp. 138–139, Apr. 1992.

[8] M. I. Aksun, S. L. Chuang, and Y. T. Lo, "Coplanar waveguide-fed microstrip antennas," *Microwave Opt. Tech. Lett.*, vol. 4, no. 8, pp. 292–295, July 1991.

[9] M. Cai, P. S. Kooi, and M. S. Leong, "Compact slot loop antenna," *Microwave Opt. Tech. Lett.*, vol. 6, no. 5, pp. 292–294, Apr. 1993.

[10] L. Rexberg, N. Dib, and L. P. Katehi, "A microshield line loop antenna for sub-mm wavelength applications," *1992 IEEE AP-S Symp. Dig.*, pp. 1890–1893.

[11] J. Laheurte, L. P. Katehi and G.M. Rebeiz, "CPW-fed active twin-slots antennas radiating through layered substrates," *1993 URSI Conf.*, pp. 14.

[12] S. C. Wu, H. Y. Yang, N. G. Alexopoulos, and I. Wolff, "A rigorous dispersive characterization of microstrip cross- and T-junctions," *IEEE Trans. Microwave Theory Techniques*, vol. 38, pp. 1837–1844, Dec. 1990.

[13] T. S. Horng, S. C. Wu, H. Y. Yang, and N. G. Alexopoulos, "A generalized method for distinguishing between radiation and surface-wave losses in microstrip discontinuities," *IEEE Trans. Microwave Theory Techniques*, vol. 38, pp. 1800–1807, Dec. 1990.

[14] W. E. McKinzie III, "Electromagnetic modeling of conductor-backed aperture antennas and circuits of arbitrary shape," Ph.D. dissertation, Univ. CA, Los Angeles, 1992.

Broadband Quasi-Microstrip Antenna

Branko D. Popović, Jon Schoenberg, and Zoya Basta Popović

***Abstract*—A new printed microwave antenna is presented. The antenna is a hybrid between a wire antenna array and a microstrip patch antenna. Although the size, cost, and efficiency are comparable to the microstrip patch, the voltage standing wave ratio 2:1 bandwidth of the antenna presented here is above 20%. The radiation pattern of the antenna does not change appreciably within the bandwidth, and the theoretical efficiency for optimal antennas remains above approximately 80% within the bandwidth. Measurements on several antennas around 2 and 4 GHz are presented, as well as theoretical results obtained using a full-wave analysis.**

I. Introduction

Microstrip patch antennas have limited bandwidths of typically a few percent, and this has been the most limiting factor for their extensive use. Various techniques for increasing the bandwidth have been used to date: reducing the Q of the circuit by reducing the substrate height and/or lowering its dielectric constant [1], using circular and square ring configurations [2], using multiple coupled resonators on the same substrate [3]–]5], using multiple vertically coupled resonators [6], and using log periodically-grated patches [7]. The largest reported bandwidths are around 20%. The disadvantages of the listed techniques include change in the radiation pattern over the bandwidth, complicated multilayer structures, and large areas taken up by the antenna. In this work, we present a new type of planar antenna [8] which is a hybrid between a wire antenna array and a microstrip patch antenna. The antenna is slightly smaller than the standard resonant patch. It exhibits a 2:1 voltage standing wave ratio (VSWR) bandwidth of about 23%, compared to only a few percent in the case of a comparable patch. The radiation pattern does not change appreciably within the bandwidth, and the polarization of the radiation field is linear with a measured cross-polarization ratios between -16 dB and -23 dB. The theoretical efficiency of these antennas when properly designed is above 80% which is higher than that of patch antennas. Rather than being resonant at a single frequency, the presented antenna has a broad resonance that can be controlled by several antenna design parameters.

Manuscript received November 12, 1993; revised July 22, 1994.

B. D. Popović is with the Department of Electrical Engineering, University of Belgrade, Yugoslavia.

J. Schoenberg and Z. B. Popović are with the Department of Electrical and Computer Engineering, University of Colorado, Boulder, CO 80309 USA.

IEEE Log Number 9414071.

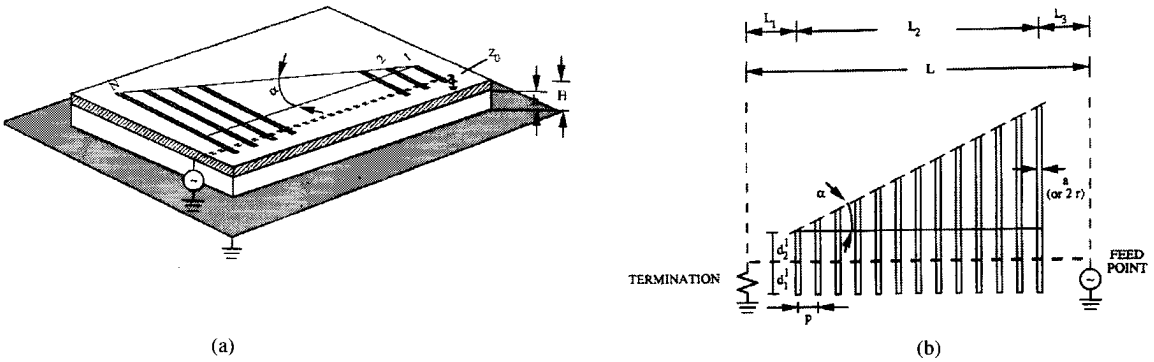

(a) (b)

Fig. 1. (a) Sketch of an N-element quasi-microstrip antenna. (b) Top view of the antenna.

II. Geometry of the Quasi-Microstrip Anisotropic Patch

The antenna is sketched in Fig. 1. It consists of a feed in the form of a microstrip line and an array of parasitic printed strips. The strips are perpendicular to, and situated above, the microstrip line. The feed line is terminated in a resistor with resistance equal to the line characteristic impedance. We call this a quasi-microstrip antenna because the planar antenna structure is less than $\lambda/10$ above the ground plane, but the antenna is a set of printed narrow strips (or wires of equivalent radius) instead of a metal patch. The antenna has an anisotropic character since the current can flow only along the thin conducting strips. The antenna has N elements with interelement spacing, p, that is much smaller than the wavelength but much larger than the strip width a (or the equivalent wire radius r). The lengths d_1^i and d_2^i of the ith element in the array are on opposite sides of the feed. The feed line is at a height h and the strips at a height H above the ground plane. The length of the printed-strip radiating array is L_2. The generator is at a distance L_3 from the longest array element and the termination at a distance L_1 from the shortest element. The taper of the "patch" width is described by the angle $\alpha = \tan^{-1}[(d_2^N - d_2^1)/L_2]$.

The antenna was analyzed and designed using the CAD program WireZeus [9]. Briefly, Hallen's generalized integral equation for the current distribution along arbitrarily interconnected straight wire segments is solved by the point-matching technique. Entire (or almost entire) domain polynomial basis functions are used for the current distribution. Each segment may have a lumped generator and/or impedance at one of its ends and may also have a distributed impedance along its length. The conductive ground plane is taken into account by the image method. In the case of narrow strips printed on an electrically thin dielectric substrate, the program analyzes approximately equivalent, magnetically coated round wires. The theory of this approximation is explained in detail in [10].

III. Experimental Models

The optimization of the heights of the substrates, h and H, was done for a single radiating strip 0.8 mm wide (i.e., for a wire 0.2 mm in radius). It was placed at the center of the feed. The impedance of the feed line alone is 283 Ω for the case of air dielectric with $h = 8$ mm. The efficiency of the feed as an antenna (with no radiating strip present) was computed as a function of h to be less than 4.4%, and the gain was less than -8 dBi. At 2 GHz, the efficiency of a single radiating strip perpendicular to and centered on a 9 cm long feed line, for $h = 8$ mm and $H = 9$ mm, as a function of the strip length is shown in Fig. 2(a). The optimal length of the radiating strip is seen to be about $0.46\lambda_0$ (i.e., approximately the first resonant length). Fig. 2(b) shows the antenna efficiency versus the feed position (in wavelengths) along the wire (i.e., d_1/λ in Fig. 1), for $(d_1 + d_2) = 7$ cm. It should be noted that the optimal feed position is quite broad, between 0.02 and 0.1 wavelength.

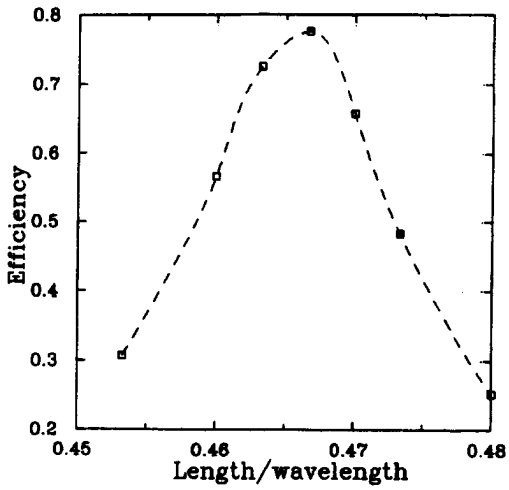

(a)

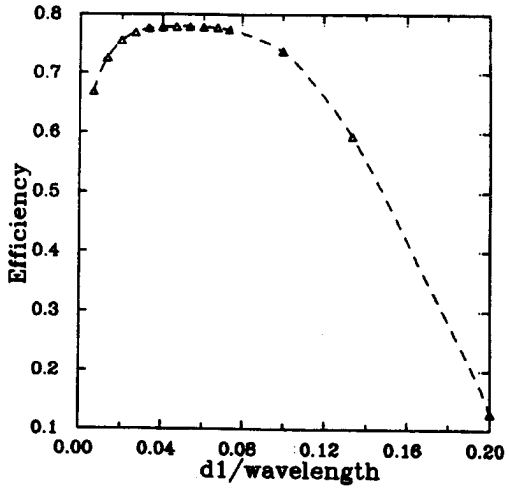

(b)

Fig. 2. (a) Efficiency of a single radiating strip 0.8 mm wide, at 2 GHz, as a function of the total strip length in wavelengths, with $d_1 = 5$ mm, $h = 8$ mm, $H = 9$ mm. (b) Efficiency of a single strip versus the position (in wavelengths) of the feed along the strip, d_1, for $d_1 + d_2 = 7$ cm, and $h = 8$ mm, $H = 9$ mm. The width of both feed and radiating strips is 0.8 mm.

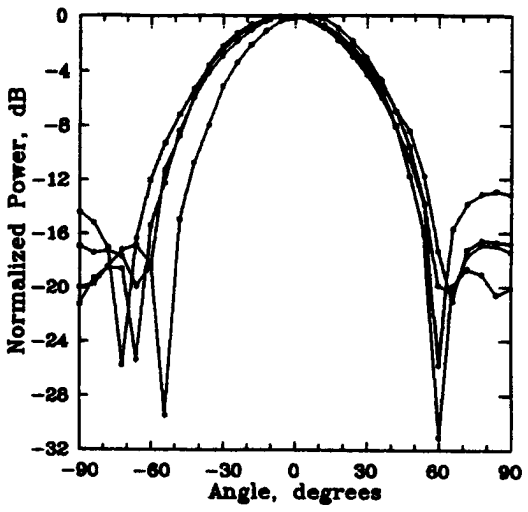

(a)

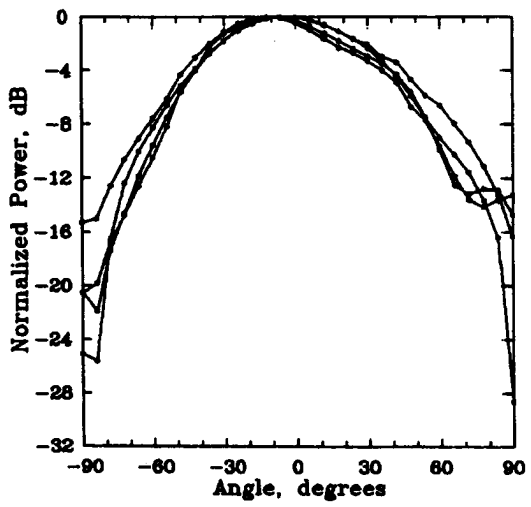

(b)

Fig. 3. Measured E-plane and (a) H-plane, (b) patterns of antenna A) at 1.5, 1.7, 1.9, and 2.1 GHz. The antenna was measured as a receiving antenna, and the received power at the measured pattern peak varied by less than 3.4 dB in this frequency range.

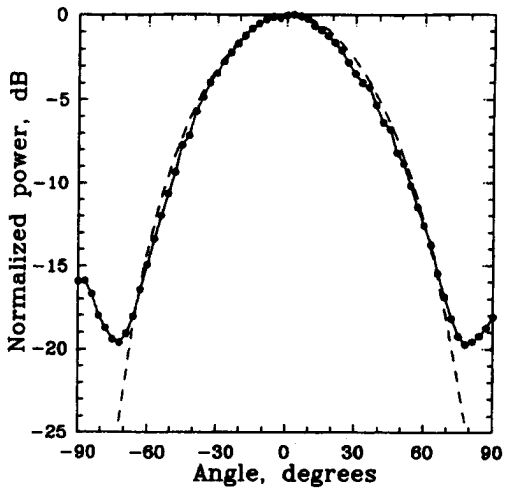

(a)

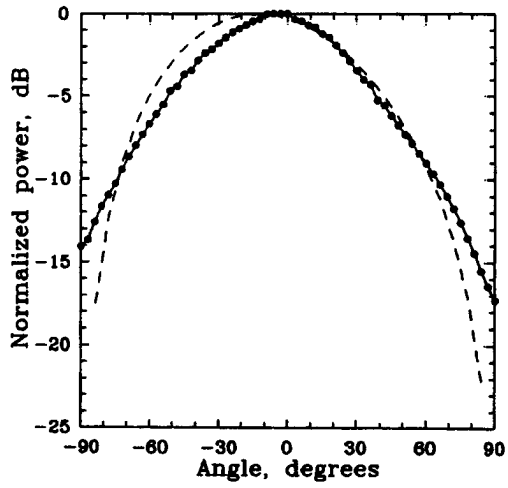

(b)

Fig. 4. Measured (solid line) and calculated (dashed line) E-plane (a) and H-plane (b) radiation patterns of antenna B) at 1.8 GHz.

As a result of these calculations, the following configurations were chosen, analyzed, fabricated, and measured:

- A) Both dielectrics are air (styrofoam), $h = 8$ mm, $H = 9$ mm, $d_1 = 10$ mm, and $\alpha = 11$ degrees. There are $N = 11$ elements and the interstrip spacing is $p = 5$ mm. The feed is #30 (AWG) wire, and the radiating strips are copper tape, 1 mm wide. The design frequency is 2 GHz. The terminating resistor is 280 Ω. The overall size (including the ground plane) is 10 cm $\times$ 9 cm which is approximately 0.4 λ_0^2.
- B) The lower dielectric is air, and the top dielectric is a Duroid substrate 0.508-mm thick with $\epsilon_r = 2.2$, $h = 8$ mm, $\alpha = 11.3$ degrees. The number of radiating strips is $N = 11$ and the period is $p = 5$ mm $= 0.03\lambda$. The feed is printed on the bottom of the dielectric substrate and the radiating strips on the top. All of the printed lines are 0.7 mm wide after fabrication. The design frequency is 1.9 GHz. A microstrip broadband matching circuit is designed for the 280 Ω termination.
- C) Essentially the same as B) but designed for operation around 4 GHz. This requires $h = 5$ mm, $H = 5.5$ mm, $d_1 = 5$ mm $\alpha = 18.4$ degrees, with a 120 Ω termination. The period is $p =$ 3 mm $= 0.04$ λ and there are $N = 13$ radiating elements. The top substrate has a permittivity of 2.2. The overall size of this antenna, including the ground plane and feed, is around 5.5 cm $\times$ 5.5 cm which is approximately $0.5\lambda_0^2$.

In models B) and C), the antenna and microstrip matching circuits were situated on the same side of the ground plane. If desired, however, the matching circuit can be located on the back side of the ground plane.

IV. Analysis and Measurements

Since no matching circuit was designed for antenna A), only radiation patterns for this antenna were measured. The measured patterns, shown in Fig. 3, practically do not change between 1.5 and 2.1 GHz which is more than a 40% bandwidth. The patterns were measured in a computer-controlled anechoic chamber with a 3-degree angular step. The antenna was measured as a receiving antenna, and the received power at the pattern peak varied by less than 3.4 dB within this bandwidth. The theoretical efficiency changes between 91% and 79% in this frequency range. With the available equipment, it was not possible to measure the full three-dimensional antenna pattern, and therefore the efficiency could not be measured.

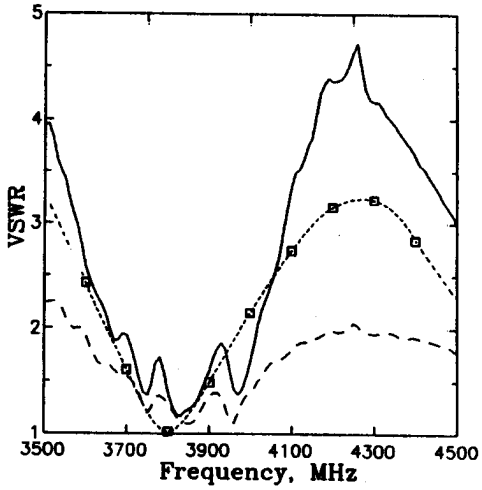

Fig. 5. Measured VSWR for antenna C) with (dashed line) and without (solid line) a microstrip-matching circuit. The dotted line shows the predicted unmatched VSWR. The 2:1 VSWR bandwidths is seen to be 23%.

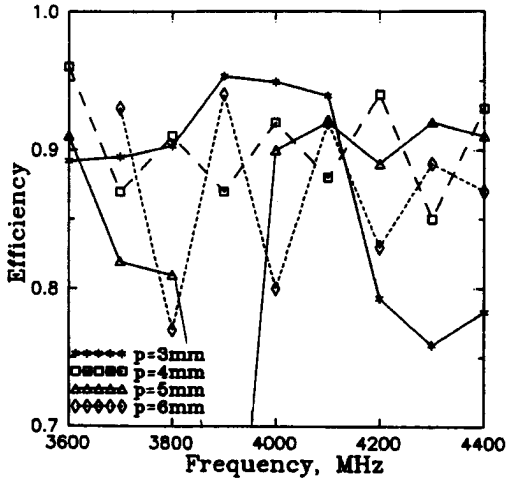

Fig. 6. The computed frequency dependence of the efficiency of the 4-GHz antenna with $N = 13$ and $\alpha = 18.4$ degrees with the inter-strip spacing, p, as parameter.

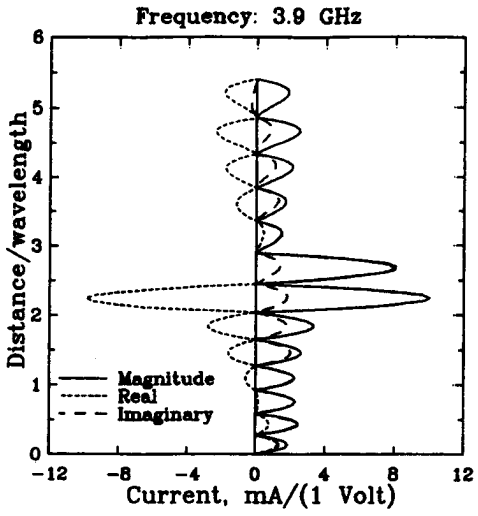

(a)

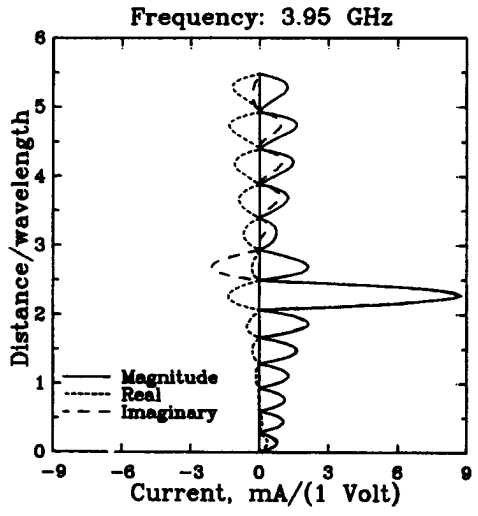

(b)

Fig. 7. Current distribution along the radiating strips of the 4 GHz antenna with $p = 5$ mm, $N = 13$ and $\alpha = 18.4$ degrees, at (a) 3.9 GHz, and (b) 3.95 GHz. The successive current bumps correspond to successive radiating strips, the longest one (i.e., the one at the generator side of antenna) being at the top of the graph.

The calculated antenna patterns agree favorably with the measured ones but are not shown in the figure for clarity.

When the generator and termination are interchanged, the efficiency and pattern degrade appreciably. The calculated efficiency then lies between 62% and 57% in the same frequency range, and the measured received power is reduced on average by 3.3 dB.

Fig. 4 shows the measured versus predicted E- and H-plane patterns for antenna B) at 1.8 GHz. The matching microstrip circuit consisted of two quarter-wave sections with impedances of 130 Ω and 57 Ω and was designed for a $s_{11} < -20$ dB between 1.8 and 2.2 GHz. This antenna exhibited a VSWR = 2:1 bandwidth of 21%, and the predicted efficiency within this bandwidth was above 80%.

Fig. 5 shows the measured and predicted VSWR of antenna C) with and without the presence of a two-section microstrip-matching circuit. With the matching circuit, the antenna has a VSWR = 2:1 bandwidth of 23%, and the predicted efficiency within the bandwidth varies between 80 and 95%. The measured and calculated radiation patterns have similar forms as those shown in Fig. 4, indicating that a typical 3-dB beamwidth for all of the presented antennas is around 60 degrees in the H-plane and 50 degrees in the E-plane. The antennas are linearly polarized with a measured crosspolarized power at the pattern peak between 16 and 23 dB below the received copolar power.

V. Discussion

There are several geometrical parameters that can be varied in the presented antenna. Although the strip width, as well as the upper substrate thickness and permittivity can also be varied, they were adopted to be 0.7 mm, 0.5 mm, and 2.2, respectively. The lengths L_1 and L_3 were also fixed at 10 mm each. The interstrip spacing, p, the number of strips, N, and the taper angle, α, for the three experimental antennas were then obtained by interactive numerical optimization. As an example, we present and discuss some of these results for the 4-GHz antenna.

The interstrip spacing (p), the number of strips (N), and the taper angle (α) were considered as parameters one at a time. (This, of course, was not a rigorous numerical optimization. Such an optimization would require simultaneous variation of all the parameters. It was found, however, that the sensitivity of the antenna properties

with the variation of one parameter was not influenced considerably by the values of the other parameters. Therefore, for engineering purposes, such an approach appeared to be satisfactory.) The number of strips was adopted to be odd with the middle strip of constant length $(d_1 + d_2) = (0.5 + 2.7)$ cm. In this manner, it was found that for the 4-GHz antenna, the conditionally optimal interstrip spacing was $p = 4$ mm, the number of strips $N = 13$, and the taper angle $\alpha = 18.4$ degrees.

In the process of optimization, a set of six parameterized graphs were obtained for the frequency dependence of the VSWR and efficiency. In these graphs, the number of elements, the interstrip spacing, and the taper were considered as parameters one at time. In addition to yielding the approximate optimal values of the parameters, this set of computed graphs pointed to some important steps in the design of such antennas. We mention here one of these as an example.

Fig. 6 shows the computed efficiency as a function of frequency for an antenna with $N = 13$ and $\alpha = 18.4$ degrees with the interstrip spacing, p, as parameter. In addition to the conclusion that the optimal value of p is between 3 mm and 4 mm, we see that, for $p = 5$ mm, the efficiency exhibits an abrupt drop at around 3.9 GHz to only about 20% (off-scale in Fig. 6). This strange behavior is due to an undesirable resonance that a good design must avoid. This resonance is best understood if one considers the current distribution along the strips at 3.9 GHz and a close frequency with normal antenna behavior. Fig. 7 shows the computed distributions at 3.9 GHz and 3.95 GHz. It is evident that at 3.9 GHz two neighboring strips form a two-wire line with large, almost equal currents in opposite direction. There is, consequently, only small radiation from these two strips. Since only these two strips are in resonance, the antenna as a whole radiates poorly. On the other hand, at 3.95 GHz only one strip is in resonance which results in efficient radiation of the antenna as a whole. All three antennas presented here were designed with this in mind. Their behavior was verified numerically in small frequency increments, but no signs of such an anomaly were observed. For a properly designed antenna, the current distribution within the operation range must look like the one in Fig. 7(b). At higher frequencies within the bandwidth of the antenna, the resonant peak moves to shorter strips (i.e., to the bottom of the figure) and at lower frequencies toward the longer strips (i.e., to the top of the figure).

REFERENCES

[1] A. G. Derneryd and I. Karlsson, "Broadband microstrip antenna element and array," *IEEE Trans. Antennas Propagat,* vol. AP-29, no. 1, pp. 140–144, Jan. 1981.

[2] W. C. Chew, "A broadband annular-ring microstrip antenna," *IEEE Trans. Antennas Propagat.,* vol. AP-30, no. 5, pp. 918–922, Sep. 1982.

[3] K. C. Gupta and G. Kumar, "Directly coupled multiple resonator wideband microstrip antennas," *IEEE Trans. Antennas Propagat.,* vol. AP-33, pp. 853–855, 1985.

[4] H. Pues, J. Bogaers, R. Pieck, and A. Van de Capelle, "Wideband quasi-log-periodic microstrip antennas," *IEE Proc.,* vol. 128, no. 3, June 1981, pp. 159–163.

[5] F. Croq and D. M. Pozar, "Multifrequency operation of microstrip antennas using aperture coupled parallel resonators," *IEEE Trans. Antennas Propagat.* vol. 40, no. 11, pp. 1367–1374, 1992.

[6] P. S. Hall, C. Wood, and C. Garrett, "Wide bandwidth microstrip antennas for circuit integration," *Electronics Lett.,* vol. 15, pp. 458–459, 1979.

[7] R. R. DeLyser, D. C. Chang, and E. F. Kuester, "Design of a log periodic strip grating microstrip antenna," *Int. J. Microwave Millimeter-Wave Computer-Aided Eng.,* vol. 3, no. 2, pp. 143–150, 1993.

[8] Z. B. Popović, E. Kuester, and B. D. Popović, "Broadband quasi-microstrip anisotropic antennas," in *IEEE APS Int. Symp. Dig.,* pp. 2073–2076, Chicago, July 1992.

[9] B. D. Popović, *CAD of Wire Antennas and Related Radiating Structures.* New York: Wiley, 1991.

[10] B. D. Popović and A. Nesić, "Generalization of the concept of equivalent radius of thin cylindrical antennas," *Proc. IEE,* Part H, vol. 131, pp. 153–158, 1984.

Unit Circle Representation of Aperiodic Arrays

Randy L. Haupt

***Abstract*—Traditionally, unit circle analysis/synthesis techniques were only applied to amplitude tapered arrays. This paper extends the method to uniformly weighted thinned and aperiodic arrays.**

I. INTRODUCTION.

An antenna array is a finite impulse-response (FIR) digital filter that samples an incident plane wave at discrete points in space. A myriad of FIR filter designs are available in which the signals at the taps (antenna elements) are weighted and combined to give a desired response. These designs have been applied to uniformly spaced antenna arrays to optimize sidelobe levels and beamwidths [1], [2]. The antenna array factor is z-transformed into a polynomial. Then, the zeros of the polynomial are represented on the unit circle in the complex plane [3]. A zero on the unit circle corresponds to a null in the antenna pattern. The placement of these zeros determines the antenna's response.

Z-transform analysis/synthesis methods rely upon an amplitude-phase representation of the array factor written as

$$F(z) = a_o + a_1 z + \cdots + a_{N-1} z^{N-1} = a_{N-1}(z - z_1) \cdot (z - z_2) \cdots (z - z_N) \quad (1)$$

where

a_n	Amplitude weight at element n.
z	$e^{j\psi}$.
ψ	kdu.
k	2π/wavelength.
d	Distance between elements.
u	$\sin\phi$.
ϕ	Angle of arrival measured from broadside.
N	Number of elements in the array.

Equation (1) is the basis for synthesizing array factors with desired directional characteristics. Relating the zeros of (1) to the zeros of a Chebychev polynomial [1] produces the familiar Dolph–Chebychev array factor with equal level sidelobe levels. Many other amplitude tapers may be derived using this method [1].

Manuscript received September 14, 1994; revised January 30, 1995.

The author is with the Department of the Air Force, USAF Academy, CO 80840–6236 USA.

IEEE Log Number 9414201.